Soft Matter

Braiding, twisting, and weaving microscale fibers with capillary forces

Journal:	*Soft Matter*
Manuscript ID	SM-ART-12-2023-001732.R1
Article Type:	Paper
Date Submitted by the Author:	15-Mar-2024
Complete List of Authors:	Sherif, Ahmed; Harvard University, School of Engineering and Applied Sciences Faaborg, Maya; Harvard University, School of Engineering and Applied Sciences Zeng, Cheng; Harvard University, School of Engineering and Applied Sciences Brenner, Michael; Harvard University, School of Engineering and Applied Science Manoharan, Vinothan; Harvard University, School of Engineering and Applied Sciences; Harvard University, Department of Physics

Braiding, twisting, and weaving microscale fibers with capillary forces

Ahmed Sherif[1], Maya Winters Faaborg[1], Cheng Zeng[1], Michael P. Brenner[1,2], Vinothan N. Manoharan[1,2*]

[1]Harvard John A. Paulson School of Engineering and Applied Sciences, Harvard University; Cambridge MA 02138 USA.

[2]Department of Physics, Harvard University; Cambridge MA 02138 USA

*Corresponding author. Email: vnm@seas.harvard.edu

Abstract

Soft materials made from braided or woven microscale fibers can display unique properties that can be exploited in electromagnetic, mechanical, and biomedical applications. These properties depend on the topology of the braids or weaves—that is, the order in which fibers cross one another. Current industrial braiding and weaving machines cannot easily braid or weave micrometer-scale fibers into controllable topologies; they typically apply forces that are large enough to break the fibers, and each machine can typically make only one topology. Here we use a 3D-printed device called a "capillary machine" to manipulate micrometer-scale fibers without breaking them. The operating principle is the physics of capillary forces: as the machines move vertically, they exert lateral capillary forces on floating objects, which in turn move small fibers connected to them. We present a new type of capillary machine that is based on principles of braid theory. It implements all the possible fiber-swapping operations for a set of four fibers and can therefore make any four-strand topology, including braids, twists, hierarchical twists, and weaves. We make these different topologies by changing the pattern of vertical motion of the machine. This approach is a mechanically simple, yet versatile way to make micro- and nano-textiles. We describe the prospects and limitations of this new type of machine for applications.

Introduction

Textiles are structured materials made from fibers.[1,2] Here we concern ourselves with two types of textiles: braids and weaves. In many applications of these textiles, it is crucial to control the topology, defined by the order in which fibers cross one another. The topology, alongside the material properties and diameters of the constituent fibers, determines the properties of the resulting textile. In particular, textiles made from micrometer- or nanometer-scale fibers can have interesting and useful mechanical or electrical properties if they have the appropriate topology. For example, Litz wire consists of conducting filaments that are braided into topologies that reduce the electrical loss.[3,4] Litz wires braided from micrometer-scale filaments could be used in a variety of applications involving electronics that operate at multi-gigahertz frequencies,[5–7] such as those used in next-generation cellular networks.

However, it is difficult to control the topology of textiles made from such small fibers. Indeed, it is difficult to even manipulate the fibers themselves. Current manufacturing methods, including

industrial maypole braiders and weaving machines, have two major limitations. First, the forces they apply are large and would break micrometer-scale fibers.[5,8–11] Second, each such machine typically makes only one topology.[12] Many techniques have been developed recently to address the first problem, manipulating small fibers without breaking them.[5,8–11,13–15] However, such techniques do not address the second problem; they are not able to make more than one topology unless they rely on a complicated mechanical setup.[16] Furthermore, many of the new techniques focus on making twists, helices, or plies of fibers[13–15] rather than the more general braids or weaves required for many applications. New self-assembly approaches[17–19] show promise for eventually addressing both problems, but here our focus is on topologies that have not yet been made through self-assembly.

We describe an approach that addresses these two problems and is based on physical principles from soft-matter physics. We 3D-print a machine[20] that consists of centimeter-scale channels. The machine is a rigid piece of plastic with no moving parts. We partially submerge the machine in a water bath and place millimeter-scale objects ("carriers") in the channels. The carriers, which are connected to micrometer-scale fibers, float at the interface and are repelled from the walls of the channels by capillary forces. As the machine moves up and down in the bath, the carriers move laterally to remain as far from the channel walls as possible. We move the device slowly enough that fluid flow does not significantly influence the motion of the carriers. Instead, the trajectories that the carriers follow are determined by the geometry of the channels. In previous work,[20] we designed and demonstrated machines with channel geometries suitable for making three-strand braids, among other topologies. However, each machine could make only one topology.

Here we describe a new approach in which the trajectories followed by the carriers can be changed depending on the history of the vertical motion of the machine, as well as the geometry of the channels. Below, we describe the operating principles in detail and show that this machine can braid, twist, and weave microscale fibers.

Background

Our "capillary machines"[20] rely on a fundamentally different linkage between the machine and the fibers than is found in industrial textile machines. In a capillary machine, forces are transmitted to the carriers by and through a fluid interface, whereas in an industrial machine, forces are transmitted through contact between moving mechanical parts and the carriers. A capillary machine therefore has a completely different design than an industrial braiding machine. In particular, a capillary machine requires only one mechanical degree of freedom (movement up and down in a bath) because the motion of the carriers is not driven by gears and tracks but instead by the variation of capillary forces within the 3D-printed network of channels. Because capillary forces are small and can be tuned over a broad range,[21–25] capillary machines are suitable for manipulating microscale fibers.

Despite these fundamental differences in operating principles and design, capillary machines and industrial textile machines can carry out similar operations on fibers. It is therefore useful to first discuss industrial braiding and weaving machines, and how their operations can be described mathematically.

Industrial maypole braiding machines use a mechanical gear system to move carriers along tracks in a certain pattern.[12] Each carrier transports one end of a fiber as it moves, so that pairs of carriers can bend fibers around each other. This crossing of fibers is the fundamental operation in making a braid. As the fibers move around one another, a take-off mechanism pulls the resulting braid away from the track, unspooling fresh fiber for continued braiding. Industrial weaving machines interlace two sets of fibers, called the warp and the weft, that are oriented perpendicularly.[26] In some industrial weaving machines, the weft fibers are inserted by fast-moving rapiers or air-jets between sets of raised and lowered warp fibers.[26,27]

We can use the mathematics of braids to describe the topologies of these textiles. Braids can be defined by the order of swaps between neighboring fibers.[28] In braid theory, each swap is represented as a generator σ_i or σ_i^{-1}, where σ_i refers to a fiber in the i^{th} position crossing over a fiber in the $(i+1)^{th}$ position and σ_i^{-1} refers to a fiber in the i^{th} position crossing under the fiber in the $(i+1)^{th}$ position. Any braid can be described by a product of generators, yielding a "braid word" that describes the sequence of swaps. The simplest way to braid hair, for example, involves dividing the hair into three sections and repeatedly swapping the first over the second and the second under the third. The braid word is $(\sigma_1\sigma_2^{-1})^m$, where m is the number of repeating units in the braid.

Any machine that braids fibers must therefore be able to swap the positions of pairs of fibers. In previous work,[20] we showed that capillary machines could accomplish this task. Specifically, we designed capillary machines that could braid fibers with diameters smaller than 10 μm into topologies described by specific braid words, such as $(\sigma_1\sigma_2^{-1})^m$. In these machines, the carriers are poly(dimethyl siloxane) (PDMS) disks that float at the air-water interface. Each carrier is pierced with a thin steel needle, which is attached to a fiber that dangles into the bath (Figure 1a). The capillary force between the wall and carriers is repulsive because the channel walls are hydrophilic, bending the interface up, while the carriers are denser than water and pin the interface, such that they bend the interface down (Figure 1a). A floating carrier therefore moves to the center of the channel to minimize the sum of the surface energy and gravitational potential energy (Figure 1b).

Repulsive capillary forces allow us to design machines that can manipulate the carriers without physical contact. We make machines with channels having cross-sections that vary with height. We move the machines vertically using a motorized stage (Figure 1c). This vertical movement of the machine changes the cross-section that the carriers interact with; in response, the carriers move to the center of the new cross-section to remain as far from the walls as possible.

Unlike traditional braiding machines, capillary machines do not have a mechanical track. Instead, the trajectories followed by the carriers on the interface depend on the shapes of the channels. For example, vertically moving a machine with a sloping channel applies lateral capillary forces that translate the carriers (Figure 2a). Furthermore, when two carriers come together, they experience a capillary attraction. When these two carriers move through a channel with a helical cross-section, the pair rotates about the point of contact (Figure 2b). By combining segments that translate and rotate with segments that separate two carriers (Figure 2c), we showed[20] that a capillary machine could perform all the motions required to swap two carriers and their attached fibers—the fundamental operation in braiding.

Because such a capillary machine applies forces only through capillary repulsion, we can control the magnitude of the forces applied to the fibers by varying parameters such as the carrier size and the channel diameter.[20] We can therefore apply forces appropriate in scale for the fibers of interest. Furthermore, such machines operate quasi-statically; we do not use or need flow to move the carriers. But because the order in which fibers are swapped depends on the order of rotators and separators, the braid topology is embedded into the hardware—that is, the structure of the channels. Therefore, the three-strand braiding machine we demonstrated in our earlier work[20] could make only one topology, that is, only one braid word. In this work, we sought to overcome this limitation.

Results and Discussion

Design principles

Here we use the braid theoretical description of topology and our physical understanding of capillary forces to design a machine that can make any *n*-strand braid of interest, including braids that have woven topologies. Instead of encoding the structure of the braid into the channel structure, we make a machine that can swap only a single pair of fibers, but in which we can choose which pair to swap based on how we move the machine up and down. In this approach, the braid topology can be programmed in software—the pattern of vertical motion that we subject the machine to.

The critical element of this machine is a "reversal-activated switch."[20] A switch consists of three channels, two of which are joined at the top and bottom to form a loop, and the third of which, the "exit channel," juts upward from this loop (Figure 3a). The operating principle of this device is, again, based on repulsive capillary forces: as the machine moves vertically, the carrier moves laterally to remain as far away from the walls as possible. Therefore, when a carrier reaches a height in the switch where two channels meet, the carrier enters the wider of the two channels. When we move the switch from top to bottom and back, the carrier enters the wider channels at the top and bottom. Consequently, it stays within the loop (Figure 3b). However, if we reverse the motion of the switch when the carrier reaches an intermediate range of heights called the "operational zone" (Figure 3c), the carrier enters the wider exit channel to stay as far from the walls as possible (Figure 3c, Supplementary Video 1).

To swap the positions of two carriers, we use a machine consisting of two switches that are placed at the same height and whose exit channels lead to a rotator (Figure 4, Supplementary Videos 2, 3, 4, 5). If we reverse the motion of the machine only when the top or bottom of the machine reaches the interface, the carriers do not swap, leaving the attached fibers unaffected (Figure 4a). If we reverse the motion of the machine when the carriers are in the shared operational zone of the switches, each carrier enters the exit channel of its switch. The machine then brings them together and rotates them about their point of contact (Figure 4b), swapping the positions of the attached fibers.

With other combinations of switches and rotators, we can control the type and position of the swaps. To make a machine that can perform both σ and σ^{-1} swaps, we place pairs of switches above and below a rotator (Figure 5a). To make a machine that can swap different pairs of fibers,

we vertically stagger multiple rotators in a machine and place pairs of switches above and below each one (Figure 5b).

A machine that can make any possible braid from four strands consists of three rotators and twelve switches, as diagrammed in Figure 5b. Above and below each rotator are pairs of switches, the positions of which are staggered so that their shared operational zones are at different heights. Reversing the machine when the carriers are in a shared operational zone above or below a specific rotator therefore affects only a neighboring pair of fibers. Reversing when the carriers are in the shared operational zone above the i^{th} rotator leads to a σ_i swap, while reversing when the carriers are in the shared operational zone below the i^{th} rotator leads to a σ_i^{-1} swap. Other patterns of vertical motion result in the identity operation (**I**). Thus, this machine can swap any neighboring pair of fibers from a set of four fibers without affecting the positions of the others.

Results from braiding fibers

We demonstrate the design principles discussed above by making a capillary machine that can make any braid topology for a set of four fibers (Figure 6). The topology is defined by the braid word, which describes the series of swaps. We execute these swaps in the order specified by the braid word by programming the vertical motion of the motorized stage holding the machine.

We start by making a braid with the topology defined by the braid word $\left(\sigma_1\sigma_2\sigma_3^{-1}\right)^m$ (Figure 7a), which is a fishtail braid with m repeating units.[29] We move the motorized stage vertically so as to reverse the machine above the first rotator, then above the second rotator, and then below the third rotator, as plotted in Figure 7b. To confirm that this pattern of vertical motion corresponds to the intended sequence of swaps, we analyze videos of the carriers to track their movement in the plane of the interface (Supplementary Video 6). Indeed, plotting the carrier positions as a function of the vertical distance traveled by the machine traces out a pattern corresponding to the fishtail braid (Figure 7c).

We then attach 5-μm-diameter Kevlar fibers to the carriers to confirm that the machine can make an actual fishtail braid. By moving the machine in the vertical pattern shown in Figure 8a, we make the braid shown in the electron micrograph of Figure 8b and represented schematically in Figure 8c. We include an animation of this process in Supplementary Video 7.

It is straightforward to make other braid topologies; to do so, we need only to reprogram the stage controller. To demonstrate, we use the same machine to make a hierarchical twist: a braid consisting of two twisted pairs of fibers that have been twisted around each other (in the opposite direction). The braid word is $\sigma_1^n\sigma_3^n\left(\sigma_1^{-1}\sigma_2^{-1}\sigma_3^{-1}\sigma_1^{-1}\sigma_2^{-1}\sigma_1^{-1}\right)^m$, where n represents the number of lower-order twists and m represents the number of higher-order twists. Other kinds of twists of small fibers can be made through self-assembly approaches;[17,18,30] we focus on the hierarchical structure because we are not aware of a self-assembly scheme that can produce it. We make this braid by moving the machine in the vertical pattern shown in Figure 8d. An electron micrograph of the resulting braid, made from 5 μm Kevlar fibers, is shown in Figure 8e, and the structure is shown schematically in Figure 8f. We include an animation of this process in

Supplementary Video 8. The hierarchical twisting approach might be used to make more complex braids for Litz wire,[3] for example.

Our approach can also make simple weaves. Although we might not think of a weave as being a braided structure, we can describe its topology as a sequence of swaps using the same notation used to describe braids. For example, in a simple or plain weave with one weft fiber and three warp fibers, the fibers go over and under one another, one at a time.[26] This topology is represented by a braid word with repeating unit $\sigma_1^{-1}\sigma_2\sigma_3^{-1}\sigma_3^{-1}\sigma_2\sigma_1^{-1}$. The corresponding pattern of vertical motion is shown in Figure 8g, an electron micrograph of an actual weave made from 5 μm Kevlar fibers is shown in Figure 8h, and the topology is shown in Figure 8i. We include an animation of this process in Supplementary Video 9.

A variation on this approach allows us to control the geometry of the fibers as well as their topology. Although the topology of the structure in Figure 8h is that of a simple weave, the geometry is different from that of a typical weave, because the two sets of fibers, the warp and the weft, are not oriented orthogonally to each other. We make an orthogonal weave by manually removing a weft fiber after each set of three swaps, adding another in its place, and continuing to weave, as shown in the diagram in Figure 9a. We use this approach to make a simple weave with three warp fibers and three weft fibers, shown in the electron micrograph of Figure 9b and rendered in Figure 9c.

Discussion

In comparison to industrial braiding machines, or even our own previously demonstrated capillary machines,[20] the approach we demonstrate here can make multiple topologies with a single machine. In principle, an *n*-strand capillary machine based on the design principles we have outlined can generate an infinite number of textile topologies, both repeating and non-repeating. Because such machines include all the generators of the braid group, making longer and more complex braid words does not require a larger or more complex machine. One needs only to control the pattern of vertical motion of the stage to vary the topology. Furthermore, for weaves, there is no theoretical restriction on how many weft fibers can be added or removed from the machine as it operates.

The current limitations of our approach are as follows. First, capillary machines of the type we demonstrate cannot yet make topologies such as knots, pseudoknots, and weaves that consist of multiple layers. However, it may be possible to make weaves that consist of multiple layers with machines that use switches to swap fibers in two-dimensional arrays. Second, we do not yet have a way to rapidly insert weft fibers between multiple warp fibers at once, as is done by the rapier or air-jet mechanisms[26,27] in industrial weaving machines. Such mechanisms may be difficult to replicate in our capillary machines because fluid drag makes it difficult to move carriers at a high speed along the interface. Third, our apparatus does not yet allow for arbitrarily long textiles. Because the fibers are cut to a fixed length before braiding, the top of the braid moves closer to the machine with each swapping operation. The fibers eventually become taut, and the resulting tension can inhibit the motion of the carriers at the interface. To avoid this problem, we use fibers that are 2–3 times longer than the width of the machine, so that they do not become taut. In future designs, it should be possible to introduce an analogue of the take-off mechanism[12] used in industrial braiding machines, which continuously unspools fiber or yarn as the braid forms.

An important distinction between our approach and that of industrial machines is that we control the geometry separately from the topology. Because tension from the fibers can restrict carrier motion, the textiles we produce must remain loose enough for the constituent fibers to move with respect to each other. However, the motion of the machine ensures the correct topology. We therefore adjust the geometry after removing the textile from the tank by, for example, pulling the fibers in a braid to adjust its pitch. In brief, capillary machines provide control over the topology but not the geometry of the textile. Control over geometry, if needed for particular applications, may require additional complexity.

For future applications, it is useful to consider how our approach scales with the number of fibers and the braid length. The volume of an n-strand capillary machine scales with n^2: the width scales linearly with n because there must be one rotator for each adjacent pair of fibers, and the height scales linearly with n because the operational zones of the switches for each rotator must not overlap. The height of a 24-strand capillary machine would be of order 1 m, a linear dimension comparable to that of a 24-strand maypole braider.[31] Nonetheless, the volume of the capillary machine would be much smaller, at least for this number of strands. It should be possible to make such a machine by 3D printing it in pieces and assembling the pieces afterward, just as we do for the four-strand machine (see Methods and Materials). We note that the comparison between the capillary and industrial machines, while useful for visualizing the relative size of a capillary machine that can operate on an industrially relevant number of fibers, may be misleading in other respects because the two types of machines serve different purposes. The capillary machine is designed to manipulate micrometer-scale fibers and to produce any braid topology. Importantly, as noted above, the size of the capillary machine does not vary with the length or complexity of the braid word.

It is also useful to examine the time required to make a textile. For a given vertical machine velocity, the time to complete each swap should scale with n, since the average distance to an operational zone increases linearly with n. Furthermore, the braiding time scales linearly with the length of the braid word. Therefore, the time required to make an n-strand braid with l swaps scales as nl. Our four-strand capillary machine produces approximately one swap per minute. By comparison, an industrial 12-strand braider can produce approximately 1000 swaps/minute.[32] Again, this comparison may be misleading in some respects, since the industrial braider cannot manipulate microscale fibers, and the applications of textiles made from microscale fibers may require only a short length of material. Furthermore, for applications it is the throughput that must be optimized. There are two ways to increase the throughput of the capillary machine. First, one can increase the vertical speed. Although we have not extensively tested the operation of the capillary machine at different speeds, we expect that the speed can be increased by at least an order of magnitude.[20] Second, one can parallelize textile production. This approach is practical because capillary machines can be produced inexpensively compared to industrial machines. Furthermore, they require only one motorized degree of freedom, so that one can place multiple copies of the same machine on a single motorized stage, and they will all execute the same operations.

Conclusions

In summary, we have demonstrated design principles for machines that can manipulate microscale fibers into arbitrary topologies using a single mechanical degree of freedom, the height of the motorized stage. We have shown that a single machine based on these design principles can produce multiple topologies of micrometer-scale Kevlar fibers, including a four-strand braid, a hierarchical twist, and a simple weave.

The design of this machine relies on two principles. The first principle is the physics of capillary forces. The shapes of the channels of the machine at any given height, along with the shape and weight of the carriers, determine the deformation of the fluid interface. Vertical movement of the machine changes the positions of the channel walls relative to the carriers, resulting in lateral capillary forces on the carriers. The deformation of the interfaces has a characteristic length scale set by the capillary length,[21] approximately 2.7 mm for an air-water interface. This macroscopic length sets the scale over which we vary the shape of our channels, and hence the size of the device. To control the magnitude of the forces applied by the machine, we can tune parameters such as the carrier weight, the carrier size, and the contact angle formed by the fluid at the machine wall.[20] Hence the physics of capillary forces enables a macroscopic machine to manipulate microscopic fibers without breaking them.

The second principle is an operating principle: controlling the vertical motion of the machine decouples the topology from the shape of the machine. By moving the machine in different vertical patterns, we can swap fibers in different orders. Any pattern of vertical motion can be programmed in software with no change needed to the hardware (the 3D-printed machine). Therefore, the machine can perform any sequence of swaps.

The unique feature of the machine we have designed is therefore that it implements all the operations within a mathematical braid group. Because the four-strand braiding machine implements all six generators of the four-strand braid group, it can be used to make any braid word in the group. There are infinitely many such braid words. However, it is useful to examine how the number of possible braids increases with the number of swaps. This problem has been examined in the mathematics literature for the specific case of the positive braid semigroups.[33,34] For four strands, the positive semigroup consists of all the braids that can be made using generators σ_1,σ_2,σ_3, but not their inverses. With 5 swaps, about 100 different braid words can be made. With 10 swaps, the number of possible braids increases to about 4000. Although these numbers are underestimates, they show how a small number of swapping operations can lead to an increasingly large space of possible outputs.

Future work might focus on the development of take-off systems like the ones used in industrial braiding machines or weft-insertion systems like the rapiers used in industrial weaving machines. The development of these auxiliary systems could open the door to making micro- and nano-textiles for electromagnetic, mechanical, or biomedical applications. We envision that such machines could be used to make Litz wire or woven micro-textiles for applications such as soft actuation[35] and smart textile wearables.[36] Other future work might focus on the development of machines that can make topologies like knots, pseudoknots, and weaves that consist of multiple layers.

Finally, we note that machines like the one we have presented could also be used to move microscopic objects along complex trajectories or to assemble such objects. Previous work in this area has shown that boundary conditions can be adjusted to manipulate the curvature of the interface and the resulting capillary forces on the particles[25,37–39]. A capillary machine presents a way to tune the boundary conditions dynamically, by adjusting the height of the machine relative to the interface. For example, we have already demonstrated that machines similar to the ones we show in this paper can be used to directly manipulate 20 μm colloidal particles[20].

Author Contributions

AS did the experiments. AS, CZ, MWF, and VNM designed the machines. AS did SEM imaging. AS, MPB, and VNM wrote and edited the paper. VNM oversaw all experimental work and preparation of the paper. MPB and VNM obtained funding.

Conflicts of interest

The authors declare the following competing interests: A patent application has been filed by CZ, MWF, AS, YBS, MPB, and VNM.

Acknowledgements

We thank Martin J. Falk, Rozhin Hajian, Ming Xiao, Amy Duwel, David J. Carter, Kasey J. Russell, Roy Gordon, Aykut Aydin, Christina Chang, Rees Garmann, and Zbigniew Rozynek for helpful discussions. This work was primarily supported by the National Science Foundation through the Harvard University Materials Research Science and Engineering Center, grant DMR-2011754. It was supported in part by the Defense Advanced Research Projects Agency (DARPA) contract FA8650-15-C-7543 to the Charles Stark Draper Laboratory. Additional support was provided by NSF through grant ECCS-1541959, the Office of Naval Research through grant number N00014-17-1-3029, and the Simons Foundation. This work was performed in part at the Harvard University Center for Nanoscale Systems (CNS), a member of the National Nanotechnology Coordinated Infrastructure Network (NNCI), funded by National Science Foundation (NSF) grant ECCS-1541959.

Data availability statement

Raw videos and experimental data are available on the Harvard Dataverse (link to be added and cited here upon acceptance).

Code availability statement

STL files are available on GitHub. Gcode scripts for automating stage motion are available on Github (link to be added and cited here upon acceptance).

Methods and Materials

To make the machines, carriers, fibers, tank, and stage, we follow the methods of our previously published work[20]. Here we summarize these methods and materials briefly, including only the details that are specific to the current study.

Preparing machines

We design machines in AutoCAD 2020 (Autodesk, Inc.). We print machines using a Formlabs Form 3 printer with Formlabs clear photopolymer resin (RS-F2-GPCL-04). After printing, we wash machines in two subsequent isopropyl alcohol baths for 15 minutes and place them in an oven at 60°C to 70°C for 30 minutes to ensure that no uncured resin remains on the completed prints. Before each experiment, we use an air plasma in a Harrick Plasma Cleaner/Sterilizer PDC-32G at high power to clean the machines and make them hydrophilic. The four-strand braiding machine used in this work is too large to print or plasma clean in one piece, and so we design it as eight separate pieces (STLs to be provided upon publication). We print and plasma clean each piece individually. Each piece has holes in the bottom (4.06 mm diameter, 5 mm depth) and posts on top (4 mm diameter, 5 mm depth) so that we can slide the pieces into each other before each experiment. To ensure that the surfaces mate and the pieces sit flat, we sand the bottom of each piece with an extra fine grit sanding sponge (3M, CP000-6P-CC).

Preparing carriers

Carriers are cut from poly(dimethyl siloxane), or PDMS (SYLGARD 184 PDMS, Dow Chemical Company). We use a 10:1 ratio of prepolymer to curing agent, to which we add food coloring (McCormick Assorted Food Color and Egg Dye, 52100071077). Typical colors used are red, blue, green, and yellow. We use a THINKY ARE-250 Mixer to mix the prepolymer, curing agent, and food coloring. We then pour a small volume of the mixed but uncured PDMS into a petri dish to form a layer 1–2 mm thick. To remove any remaining gas bubbles in the PDMS mixture, we vigorously tap the petri dish against a flat surface. We then cure the PDMS in an oven for several hours at 60°C to 70°C. In this work, we use circular carriers with diameter 3 mm, which we cut from the PDMS using surgical hole punches made by World Precision Instruments (WPI, Item No. 504649). Cured PDMS has a specific gravity of 1.03 @ 25°C, according to the SYLGARD 184 technical data sheet. The PDMS carriers are thus slightly denser than water.

Preparing fibers

In this work, we use 5 μm diameter Kevlar fibers purchased from The Thread Exchange (KEV000BLAC02w). As noted in our previous paper, the fiber length should be chosen to keep the fibers slack during the entire braiding process, so that they can easily be bent around one another.[20] Here we cut the fibers to a length of 15 cm, which allows us to make braids that are 10–20 swaps long without the fibers becoming taut. To make longer braids, one must use a longer fiber. To make braids from stiffer fibers, one can use a longer fiber to reduce the bending stiffness, which scales with the inverse cube of the fiber length, as discussed in the

Supplementary Information of our previous paper.[20] We attach fibers to the carriers by gluing (Gorilla Glue, GOR7500101) one end to thin carbon fiber rods (McMaster-Carr, Catalog No. 2004N11, diameter 0.27 mm). The carbon fiber rods we use are 20–24 cm long, such that they pass through the full height of the machine, allowing the fibers to move without touching the channel walls. All machines contain slots that allow the rods to pass through the machines as the rods move with the carriers. We pierce the center of each PDMS carrier with a carbon fiber rod. To anchor the fibers, we glue a small plastic washer (McMaster-Carr, Catalog No. 93493a343) to the free end. After waiting 30 min for the glue to dry, we place the carriers and attached fibers in a tank of water. The carriers are held in straight 3D-printed channels in our stage. We hook the washers on a post that we fix to the bottom of the tank, approximately 5 cm in front of where the machine is placed on the stage. For experiments involving weaving, we fix multiple posts to the bottom of the tank and hook the washers corresponding to warp and weft fibers to distinct posts. This approach makes it easier to distinguish between the different sets of fibers. While weaving, we add and remove weft fibers manually when the carriers are at the base of the machine.

Tank and stage

The water tank is made from 0.5 cm thick acrylic (PMMA) plastic sheets and has dimensions 29 × 28 × 41 cm. We fill it with approximately 6 gallons of clean, distilled water (Poland Spring). The stage consists of several pieces of laser-cut PMMA sheets that are secured to one another with nuts and bolts (McMaster-Carr 18-8 Stainless Steel Socket Head Cap Screw, part number 92196A230, and 18-8 Stainless Steel Hex Nuts, part number 91841A155). The stage is moved by a stepper motor (Nema 17 42HD4027-36) with a threaded shaft. The stage moves vertically and can be programmed to reverse direction at any point. We use Gcode (a computer numerical control programming language) scripts to automate the stage (scripts to be provided upon publication). Typical stage speeds are 50-100 mm/min. Dimensional diagrams of the tank and stage can be found in our previous work.[20]

In this work, the base of the stage is a 3D-printed part with a cross-section identical to the base of the four-strand machine (STL files to be shared upon publication). The base is attached to the rest of the stage by four steel bars (5 mm diameter) that fit into side arms on the side of the part. To load fibers into the machine, we place the carriers in these channels and then place the machine on top of the stage. We then lower the stage such that base of the machine is level with the water-air interface. We then start the Gcode script that automates the vertical motion of the stage. For experiments that do not involve fibers (Figure 4), we place the machine so that its top is level with the interface, and we move the machine up. For experiments that involve braiding or weaving (Figures 7, 8), we place the machine so that its base is level with the interface and move the machine down.

Imaging

We image braided and woven microscale fibers with a Zeiss FESEM Ultra Plus. We use an Everhart-Thornley (SE2) detector. Typical settings are 2.00 kV EHT, 100× magnification, 12 mm working distance. Before imaging, we sputter-coat samples with a Pt/Pd 80-20 alloy in an EMS Sputter Coater.

Top-view and side-view videos of the machines are taken with an iPhone 8 camera.

Rendering

Supplementary Videos 7, 8, and 9 include 3D renderings of the braiding, twisting, and weaving process. These renderings are included to illustrate how the motion of the carriers at the interface and the changing vertical motion of the machine can result in different topologies. These renderings were made using Blender (3.3.1). To render the fibers as they are being braided, we applied Blender's soft body physics and collision physics modifiers to subdivided and loop-cut cylindrical meshes. The ends of the cylindrical meshes are hooked to move along with the carriers. The carrier motions are manually programmed.

References

1 S. V. Lomov, G. Huysmans and I. Verpoest, *Textile Research Journal*, 2001, **71**, 534–543.

2 S. V. Lomov, G. Huysmans, Y. Luo, R. S. Parnas, A. Prodromou, I. Verpoest and F. R. Phelan, *Composites Part A: Applied Science and Manufacturing*, 2001, **32**, 1379–1394.

3 G. W. O. Howe and T. Mather, *Proceedings of the Royal Society of London. Series A, Containing Papers of a Mathematical and Physical Character*, 1917, **93**, 468–492.

4 W. G. Hurley, M. C. Duffy, J. Acero, Z. Ouyang and J. Zhang, in *Power Electronics Handbook*, Elsevier, 2018, pp. 571–589.

5 J. P. Phillips, US Pat., US 8,017,864 B2, 2011.

6 M. J. Schulz, B. Ruff, A. Johnson, K. Vemaganti, W. Li, M. M. Sundaram, G. Hou, A. Krishnaswamy, G. Li, S. Fialkova, S. Yarmolenko, A. Wang, Y. Liu, J. Sullivan, N. Alvarez, V. Shanov and S. Pixley, in *Nanotube Superfiber Materials*, eds. M. J. Schulz, V. N. Shanov and Z. Yin, William Andrew Publishing, Boston, 2014, pp. 33–59.

7 A. Aydin, Ph.D. Thesis, Harvard University, 2019.

8 P. Marchand, J. Nolting, D. J. Kent, T. Q. Dinh, H. P. Tran, J. Milburn and J. Thompson, US Pat., US8261648B1, 2012.

9 S. Giszter, T. G. Kim and A. Ramakrishnan, US Pat., US8534176B2, 2013.

10 A. Duwel, J. LeBlanc, D. J. Carter and E. S. Kim, US Pat., US20170058440A1, 2017.

11 R. Quick, C. Thress and G. Ulrich, US Pat., US20200240056A1, 2020.

12 Y. Kyosev, *Braiding technology for textiles*, Woodhead Pub, Waltham, MA, 2014.

13 M. Zhang, K. R. Atkinson and R. H. Baughman, *Science*, 2004, **306**, 1358–1361.

14 H. K. Murnen, A. M. Rosales, J. N. Jaworski, R. A. Segalman and R. N. Zuckermann, *J. Am. Chem. Soc.*, 2010, **132**, 16112–16119.

15 Y. Lu, X. Cheng, H. Li, J. Zhao, W. Wang, Y. Wang and H. Chen, *J. Am. Chem. Soc.*, 2020, **142**, 10629–10633.

16 A. A. Head and V. M. Ivers, US Pat., US20160083879A1, 2016.

17 D. M. Barber, T. Emrick, G. M. Grason and A. J. Crosby, *Nat Commun*, 2023, **14**, 625.

18 D. M. Hall, I. R. Bruss, J. R. Barone and G. M. Grason, *Nature Mater*, 2016, **15**, 727–732.

19 B. Pokroy, S. H. Kang, L. Mahadevan and J. Aizenberg, *Science*, 2009, **323**, 237–240.

20 C. Zeng, M. W. Faaborg, A. Sherif, M. J. Falk, R. Hajian, M. Xiao, K. Hartig, Y. Bar-Sinai, M. P. Brenner and V. N. Manoharan, *Nature*, 2022, **611**, 68–73.

21 P.-G. de de Gennes, F. Brochard-Wyart and D. Quere, *Capillarity and Wetting Phenomena: Drops, Bubbles, Pearls, Waves*, Springer-Verlag, New York, 2004.

22 D. Vella and L. Mahadevan, *American Journal of Physics*, 2005, **73**, 817–825.

23 I. Ho, G. Pucci and D. M. Harris, *Phys. Rev. Lett.*, 2019, **123**, 254502.

24 I. B. Liu, N. Sharifi-Mood and K. J. Stebe, *Annu. Rev. Condens. Matter Phys.*, 2018, **9**, 283–305.

25 N. Sharifi-Mood, I. B. Liu and K. J. Stebe, *Soft Matter*, 2015, **11**, 6768–6779.

26 S. Adanur, *Handbook of Weaving*, CRC Press, Boca Raton, 2020.

27 T. Kinari, *Journal of Textile Engineering*, 2007, **53**, 43–52.

28 E. Artin, *Annals of Mathematics*, 1947, **48**, 101–126.

29 L. Hu, C. Ma, L. Luo, L.-Y. Wei and H. Li, *ACM Trans. Graph.*, 2014, **33**, 225:1-225:9.

30 G. M. Grason, *Soft Matter*, 2020, **16**, 1102–1116.

31 A. Bicking, Masters thesis, North Carolina State University, 2011.

32 S. Omeroglu, *Fibres & Textiles in Eastern Europe*, 2006, **14**, 53–57.

33 P. Xu, *Journal of Pure and Applied Algebra*, 1992, **80**, 197–215.

34 Z. Iqbal, *Algebra Colloq.*, 2011, **18**, 1017–1028.

35 A. Maziz, A. Concas, A. Khaldi, J. Stålhand, N.-K. Persson and E. W. H. Jager, *Science Advances*, 2017, **3**, e1600327.

36 M. Martínez-Estrada, H. Ventura, I. Gil and R. Fernández-García, *Advanced Materials Technologies*, 2023, **8**, 2200284.

37 A. Read, S. K. Kandy, I. B. Liu, R. Radhakrishnan and K. J. Stebe, *Soft Matter*, 2020, **16**, 5861–5870.

38 I. B. Liu, N. Sharifi-Mood and K. J. Stebe, *Philosophical Transactions of the Royal Society A: Mathematical, Physical and Engineering Sciences*, 2016, **374**, 20150133.

39 L. Yao, N. Sharifi-Mood, I. B. Liu and K. J. Stebe, *Journal of Colloid and Interface Science*, 2015, **449**, 436–442.

Figures

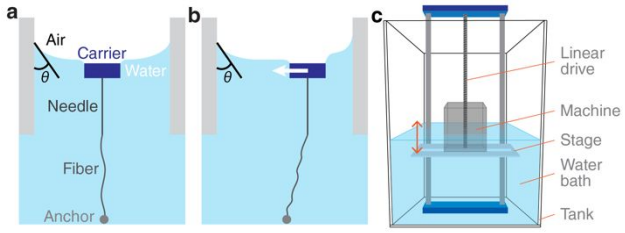

Figure 1. Capillary machines rely on repulsive capillary forces to move floating objects. (a) Cross-sectional diagram of a plastic channel of a capillary machine. The hydrophilic channel wall meets the interface at a contact angle θ. The carrier is a PDMS disk that, being denser than water, bends the interface downward. The carrier moves to the center of the channel to minimize the sum of the interfacial energy and gravitational potential energy. We pierce each carrier with thin steel needles to which we glue one end of a fiber. The other end of the fiber is anchored. The position of one end of the fiber is thus controlled by the position of the carrier at the interface. (b) If the carrier is perturbed away from the center of the channel, the interfacial and gravitational potential energies increase, resulting in a restoring force (white arrow). We use this principle to manipulate carriers by making machines with cross-sections that vary with height. Such machines present a different boundary to the carriers depending on their vertical position. (c) Diagram of apparatus for moving capillary machines into and out of water. We place the machines on a stage in a tank of distilled water. The stage moves vertically and can be programmed to reverse direction at any point.

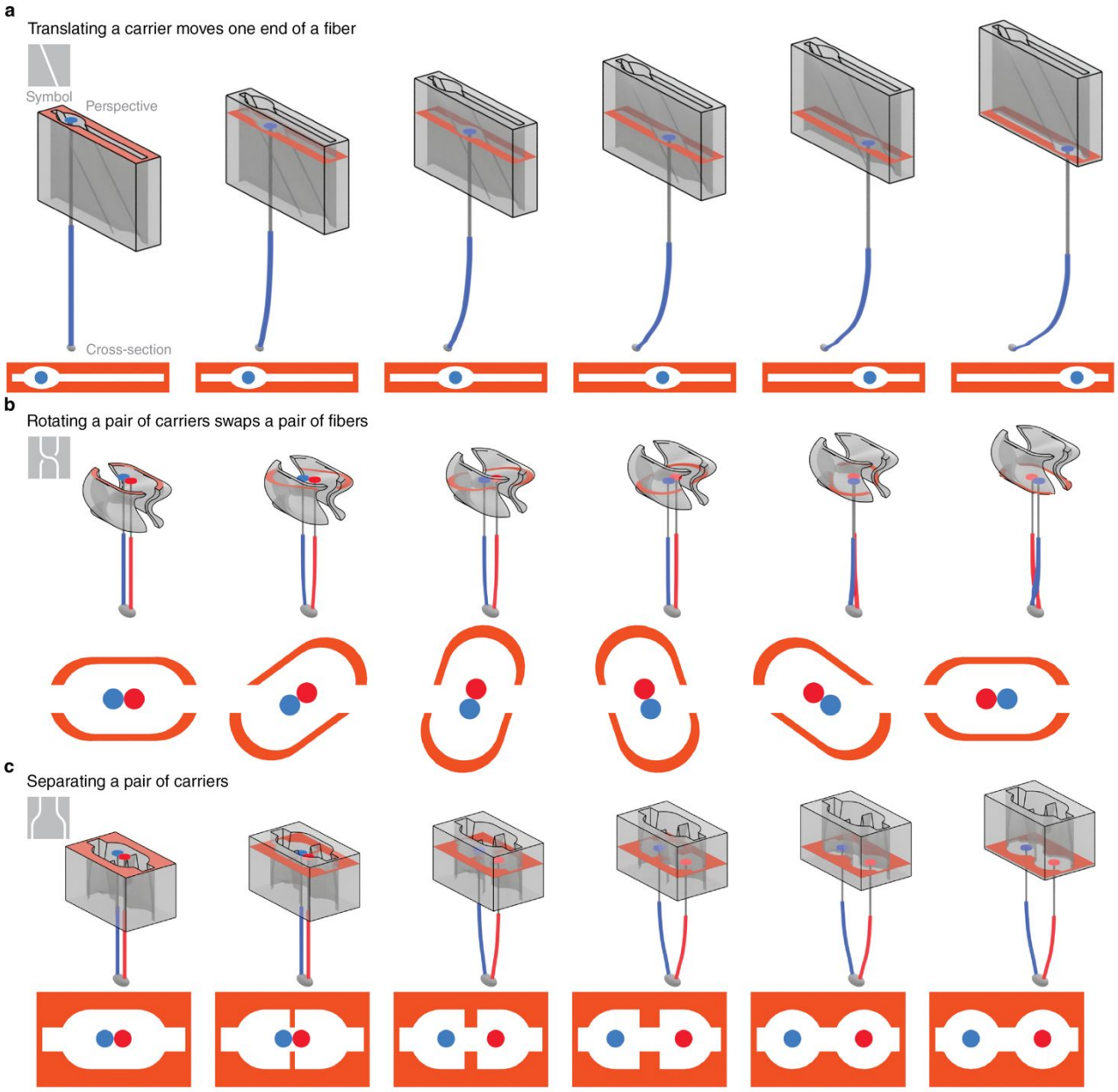

Figure 2. Elementary capillary machines that can manipulate carriers and fibers. In each of the diagrams, the orange shaded area shows the cross-section of the machine that is level with the water-air interface. Moving the devices vertically changes the cross-section that the carriers (blue and red) interact with. In response, they move to stay as far from the walls of the channel as possible. (a) A machine (shown in a perspective rendering, top, and cross-section rendering, bottom) that consists of a sloping channel translates a carrier and an attached fiber (blue curve)

as it moves vertically with respect to the interface. (b) A machine that consists of oval cross-sections that twist with height rotates a pair of carriers and attached fibers (blue and red curves) as it moves vertically. The rotation of the carriers at the interface swaps the positions of the attached fibers. (c) A machine that consists of wedged channels separates a pair of carriers. Separating carriers after swapping allows them to return to their initial positions for subsequent swapping operations.

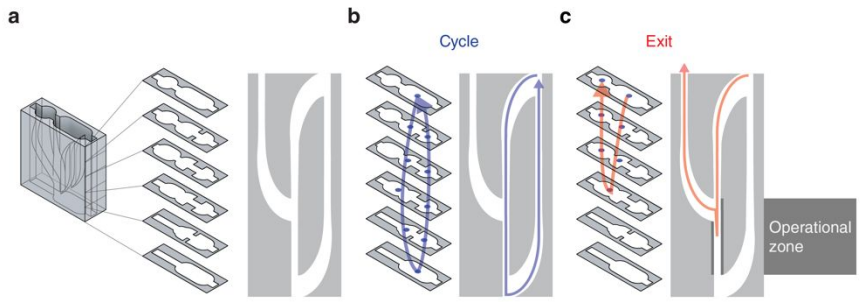

Figure 3. A reversal-activated switch. (a) At left, perspective rendering and cross-sections of the switch. The switch allows us to program multiple paths of motion into a single machine. As shown in the schematic at right, it consists of three channels of varying width, two of which are joined at the top and bottom and the third of which, the "exit" channel, juts out of the loop formed by the first two. One can predict the motion of a carrier relative to the machine by tracing a path through the schematic. In the frame of the machine, this path is always in the direction opposite the motion of the stage. Whenever the stage reverses direction, and there are two channels presented to the carrier, it enters the wider channel to remain as far away from the walls as possible. (b) Rendering of cross-sections of the switch (left) and schematic, showing the path of a carrier (blue lines) when the switch moves in a full cycle, only reversing its direction at the top and bottom. The carrier moves in a cyclical path. (c) As in panel b, but showing the path of the carrier (orange lines) when the motion of the machine is reversed within the operational zone, indicated by the dark gray lines. In this case, the carrier enters the exit channel.

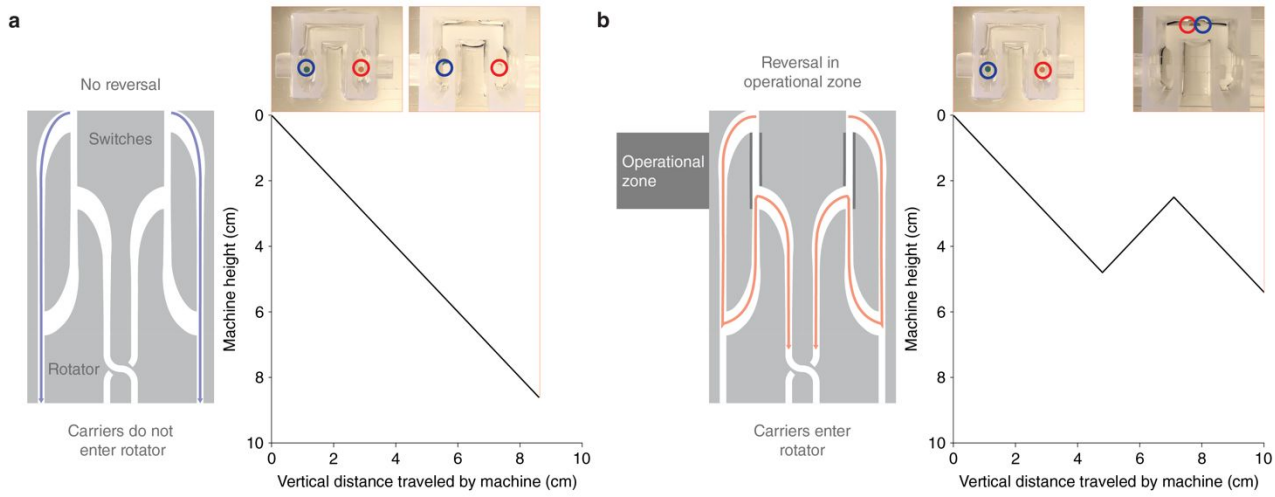

Figure 4. Using switches to swap the positions of carriers. (a) At left, schematic of a machine that consists of two reversal-activated switches and a rotator. Here the switches are oriented such that their exit channels lead down to a rotator and their operational zones are at the same height. If the motion of this machine is not reversed, the carriers do not swap positions, as shown by the blue paths. Right, top-view photographs of the machine and carriers at the beginning and end of a trajectory in which the motion is not reversed. The carriers (circled in red and blue for clarity) remain in their initial position. Below, a plot of the height of the machine with respect to the vertical distance it travels. (b) Same as for panel a, but when the motion of the machine is reversed when the carriers are in the operational zone of the pair of switches. The orange path in the left diagram shows the motion of the carriers. To ensure that the carriers go into the rotator from above, the machine must reverse twice: once before the operational zone, and once inside the operational zone. These reversals are seen in the plot at right. Reversing in the operational zone causes the carriers to enter the exit channels, enter the rotator, and swap positions, as shown in the top-view photographs.

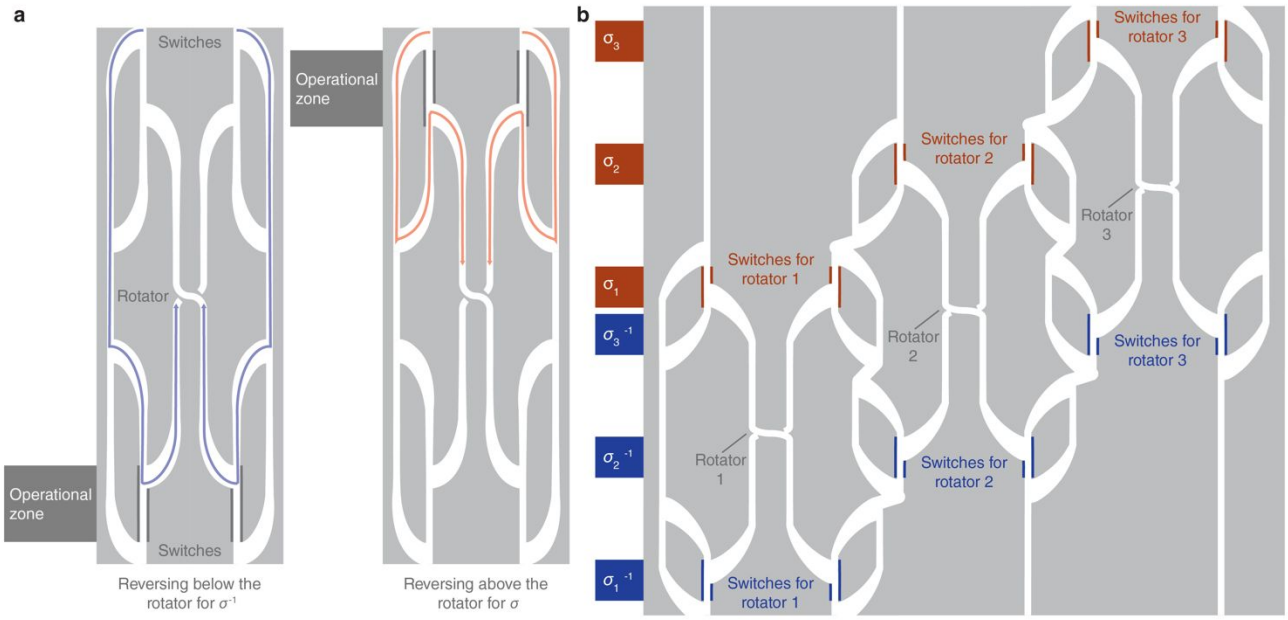

Figure 5. Vertically staggered switches enable swapping multiple pairs of fibers. (a) Schematic of a machine that can execute both σ swaps and σ^{-1} swaps. The machine consists of one rotator, with pairs of reversal-activated switches above and below. Reversing the motion of the machine when the carriers are in the operational zone below the rotator (blue lines in left diagram) executes a σ^{-1} swap. Reversing the motion of the machine when the carriers are in the operational zone above the rotator (orange lines in right diagram) executes a σ swap. Separators (not shown) above and below the rotator separate the carriers from each other after swapping. (b) A schematic of a four-strand braiding machine that consists of three rotators and pairs of switches above and below each rotator. The height of the shared operational zones of each pair of switches is represented by the dark blue and red lines in the schematic and flags at left. The switches are vertically staggered so that there is no overlap between the shared operational zones of each pair of switches. Reversing in the shared operational zone above the i^{th} rotator executes a σ_i swap, while reversing in the shared operational zone below the i^{th} rotator executes a σ_i^{-1} swap.

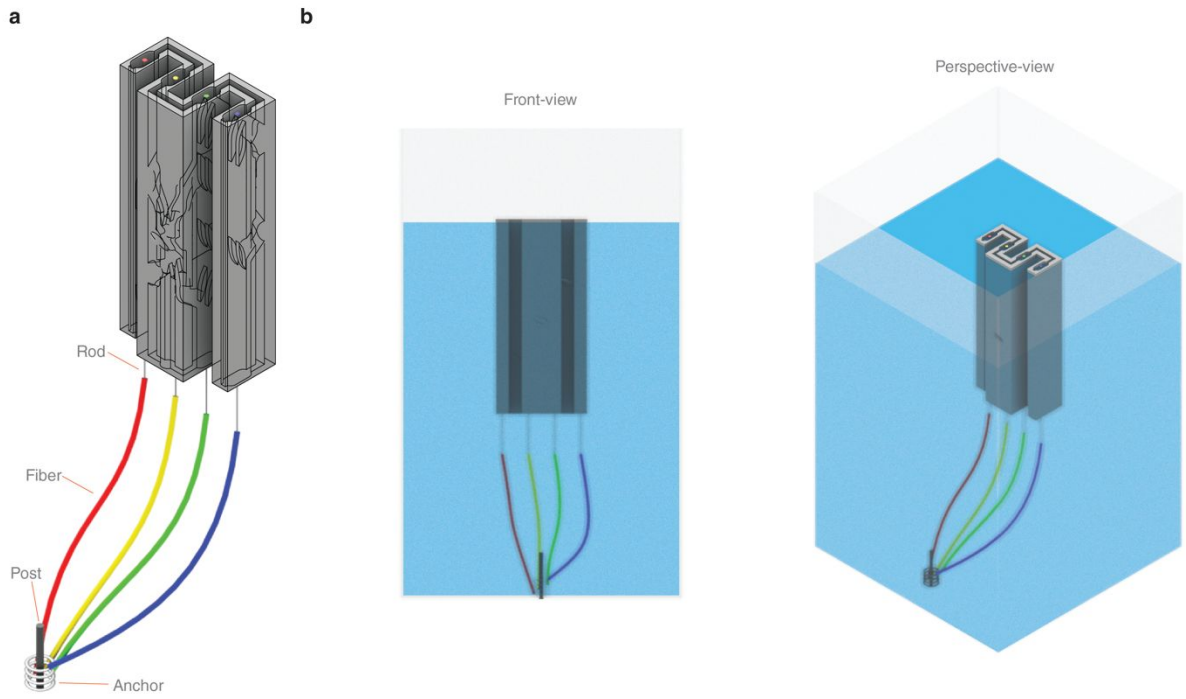

Figure 6. Rendering of a four-strand braiding machine in a tank of water. (a) Fibers are connected to the carriers (red, yellow, green, and blue circles at the top of the machine) by thin carbon fiber rods. The free ends of the fibers are anchored to the bottom of the tank by small plastic washers placed on a post. (b) Front-view and perspective-view renderings of the braiding machine and fibers in a tank of water (stage not shown).

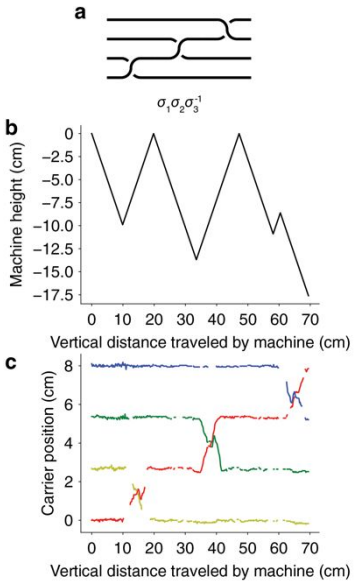

Figure 7. With the appropriate sequence of swaps, the motion of the carriers traces out a fishtail braid. (a) Braid diagram and braid word for a fishtail braid, showing the sequence of swaps in the repeating unit. (b) A plot of machine height with respect to vertical distance traveled by the machine. Each extremum represents a reversal in the motion of the machine. (c) A plot of the measured carrier positions with respect to vertical distance traveled by machine, showing three swaps. Each swap happens after a reversal.

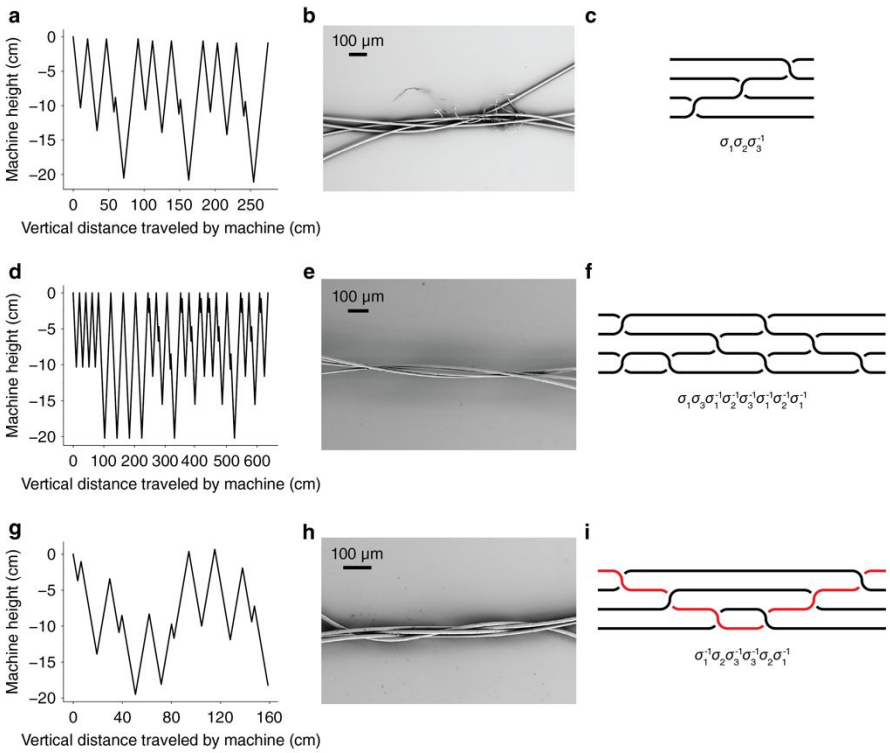

Figure 8. Results from using the machine to braid, twist, and weave microscale fibers. (a) Plot of machine height with respect to vertical distance traveled by machine. (b) Scanning electron micrograph of a fishtail braid made from microscale Kevlar fibers. The smaller fibers in this micrograph are likely dust or fibers from paper that were caught between the Kevlar fibers. (c) Braid diagram of fishtail braid. (d, e, f) As in panels a,b,c but for a hierarchical twist. (g, h, i) As in panels a,b,c but for a simple or plain weave. The weft fiber is indicated in red.

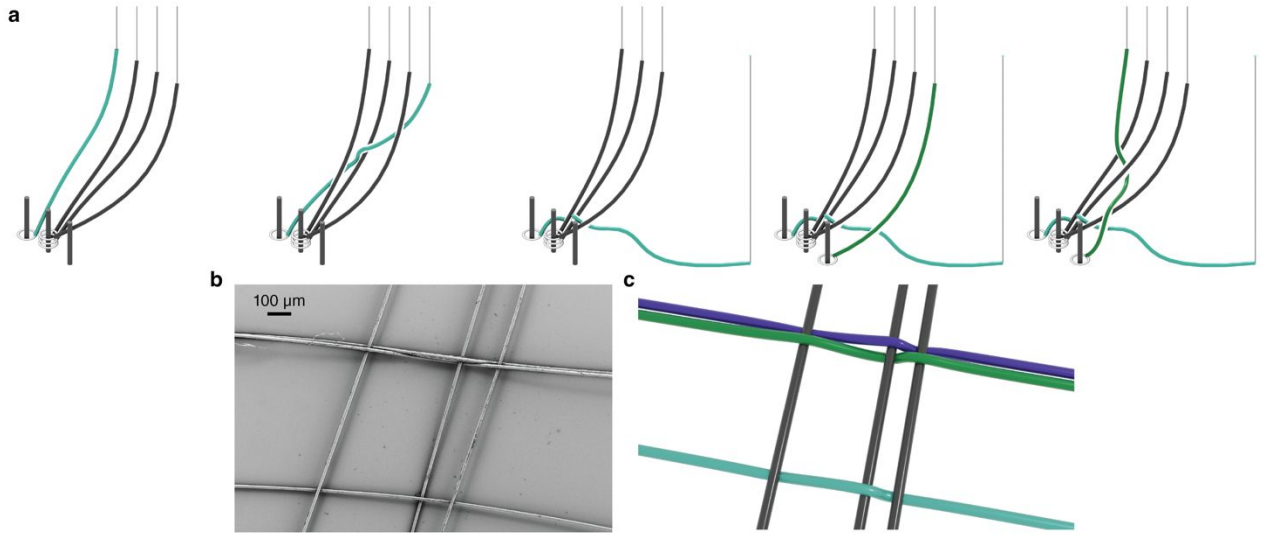

Figure 9. Process for adding weft fibers into capillary machine. (a) Diagrams showing steps of a process for adding and removing weft fibers. We start with one weft fiber (teal). Then, the machine weaves the weft fiber through the three warp fibers (gray). We then remove the weft manually from the machine. Next, we manually add a new weft fiber (green) in the original weft fiber's place. We continue weaving with this fiber. Each of the addition and removal steps is done when the machine is at its maximum height and the fluid interface is at the bottom of the machine. We can repeat this process to continue adding weft fibers. After we finish weaving, we pull the fibers to adjust the orientation between the warp and weft fibers. (b) Scanning electron micrograph of a simple or plain weave with three warp fibers and three weft fibers. (c) Rendering of the image in panel b, to indicate which of the fibers in the micrograph are warp fibers (rendered in gray) or weft fibers (rendered in teal, green, and blue).

Descriptions of videos

Video 1: Perspective rendering and rendering of the cross-section of the machine at the height of the interface of a reversal-activated switch as it moves in a cycle and as it reverses direction in an operational zone.

Video 2: Top-view video of a machine that consists of two switches and one rotator as it moves vertically without reversing. Video sped up by a factor of 5.

Video 3: Top-view video of a machine that consists of two switches and one rotator as it reverses direction while moving vertically. Video sped up by a factor of 5.

Video 4: Perspective rendering and rendering of the cross-section of the machine at the height of the interface of a machine that consists of two switches and one rotator as it moves vertically without reversing.

Video 5: Perspective rendering and rendering of the cross-section of the machine at the height of the interface of a machine that consists of two switches and one rotator as it reverses direction while moving vertically.

Video 6: Front-view video of a four-strand braiding machine moving in the pattern that creates a four-strand fishtail braid. Video sped up by a factor of 5.

Video 7: Perspective and front-view rendering of a four-strand braiding machine as it makes a fishtail braid. This video is for illustration and does not represent a physical simulation; the deformations of the fibers are an artifact of the rendering process.

Video 8: Perspective and front-view rendering of a four-strand braiding machine as it makes a hierarchical twist. This video is for illustration and does not represent a physical simulation; the deformations of the fibers are an artifact of the rendering process.

Video 9: Perspective and front-view rendering of a four-strand braiding machine as it makes a simple weave. This video is for illustration and does not represent a physical simulation; the deformations of the fibers are an artifact of the rendering process.